DOE/ET-53088-389 IFSR #389

Two-stream Instability Threshold of the Migma Exyder

O. Ågren, H.L. Berk, and *H.V. Wong*
Institute for Fusion Studies
The University of Texas at Austin
Austin, Texas 78712

August 1989

Two-stream Instability Threshold of the Migma Exyder

O.Ågren, H.L. Berk and H.V. Wong,

Institute for Fusion Studies, The University of Texas at Austin,
Austin, Texas 78712.

Abstract: The response to electrostatic perturbations, $\phi = \hat{\phi}(r,z)e^{i(l\theta - \omega t)}$, in the Migma Exyder is investigated. The ions are modelled as a relativistic mono-energetic distribution with a small spread in the impact parameter (the distance of closest approach to the axis) and with the axial extent ΔZ much shorter than the radial extent R_0. It is found that odd l-modes do not give rise to a low-frequency response. For $l = 0$, an energy principle for low-frequency ion-ion interactions is formulated, and it is shown that the extremizing perturbation is located to a narrow region surrounding the axis. The threshold is proportional to the total number of stored particles, $N = 4\varepsilon_0(\pi - 2)\gamma(\gamma^2 - 1)m_i c^2 R_0/q_i^2$ where γ is the usual relativistic factor, and this stability condition therefore allows for a high density on axis in highly focused systems. Compared to a cylindrical shape, a disk-shaped plasma gives an improvement in the density by the factor $R_0/\Delta Z$. The threshold in particle number for the relativistic ion-ion two-stream instability scales as γ^3 thus with relativistic effects the instability is further suppressed. Inclusion of the electron response increases the threshold even further. Preliminary investigations indicate that finite frequency modes can give a lower threshold than the zero frequency case, at least for nonrelativistic beam energies. An uncertainty arises because the variational procedure is less accurate for the finite frequency case. These finite frequency instabilities can arise from coupling between positive and negative energy modes.

I. Introduction

Blewett[1] has recently proposed a modification of the coil configuration for the generation of the magnetic field in migma systems. He showed that one can design vacuum magnetic field coils where the magnetic field is low on axis and large at a radius $r \approx r_1$. A suitable design of the magnetic field will focus orbits radially and axially[2,3] (see Fig.s 1a and 1b).

As in the original migma concept, the intention with this so called Migma Exyder is to create from a self-colliding beam a plasma where the ions passes close to the axis in each radial bounce[4]. The shape of some particle orbits in the (x,y) plane is outlined in Fig.2a. Besides the possible relevance in fusion research, the Migma Exyder has also interest as a storage ring for high energy particles, provided good axial confinement and a high luminosity can be created near the axis.

In any migma system with convergent beams, there may be a potential danger for onset of two-stream instabilities, which would broaden the distribution in the impact parameter. Gnavi and Gratton have investigated two-stream ion-ion[5] and ion-electron[6] instabilities in cylindrical geometry for a perfectly focused beam, i.e., $P_\theta = 0$. They showed that an ion-ion two-stream instability is present in their model when $R_0 > v_i / \overline{\omega}_{pi}$ where $\overline{\omega}_{pi}$ is the plasma frequency averaged over the ion extent, v_i the ion speed and the ions are contained in a cylinder of radius R_o. They calculate growth rates when $R_0 > v_i / \overline{\omega}_{pi}$, but only estimate the threshold density of instability.

Here we develop a kinetic theory for small but finite P_θ and consider a configuration where the axial extent is much less than the radial extent, i.e., a disk-shaped instead of a cylindrically shaped plasma is considered. We derive and analyze a quadratic dispersion functional for the pure ion-ion streaming instability and then extent the analysis to include electron-ion interactions.

II. Orbits in the Equilibrium

A disk-shaped plasma where relativistic ions are axially focused but otherwise have negligible axial velocity is considered. To model the two-stream effect in the Migma Exyder, the ion orbits are approximated with straight lines in the weak field region $r < R_0$. By assuming that the reflection region $r \gtrsim R_0$ is not essential for the two-stream effect, it is appropriate to model the system with $B = 0$ for $r < R_0$ and $B \longrightarrow \infty$ for $r > R_0$, in other words instantaneous reflection is assumed when the ions reach $r = R_o$ (see Fig.2b). Inside the containment region, the magnetic field is considered negligible for the ions. However the B-field can still be large enough to be important for the electron dynamics. We shall consider the electron Larmor radius much less than the system size, and for most of the work we also consider $\omega_{ce} \equiv eB/m_e > \omega_{pe} = e(n/m_e\varepsilon_0)^{1/2}$ and $\omega_{ce} > |\omega|$ in which case electrons can be disregarded. However, in later part of this work we reanalyze stability when ω_{ce}/ω_{pe} is arbitrary.

The energy $H = \gamma m_i c^2$ and the canonical momentum $P_\theta = \gamma m_i r v_\theta$ are constants of motion. It is convenient to express the equilibrium distribution function in terms γ and the impact parameter b

$$f(\mathbf{r},\mathbf{v}) = F(\gamma,b)\delta(v_z) \tag{1}$$

$$\gamma = \frac{H}{m_i c^2} = \frac{1}{m_i c^2}\sqrt{m_i^2 c^4 + c^2 P_r^2 + c^2 \frac{P_\theta^2}{r^2}} \tag{2}$$

$$b = \frac{cP_\theta}{\sqrt{H^2 - m_i^2 c^4}} = \frac{P_\theta}{m_i c\sqrt{\gamma^2 - 1}} \tag{3}$$

The closest approach to the axis for the particle is $|b|$. By evaluating the Jacobian of the transformation $(\gamma v_r, \gamma v_\theta) \longrightarrow (\gamma, b)$, the expressions for the line integrated density $n(r) = \int n_v(r,z)\, dz \approx n_v \Delta Z$ (n_v is the volume density) and the total number of particles are found to be

$$n(r) = 2c^2 \int_{-r}^{r} db \int_1^{\infty} d\gamma \, \frac{\gamma}{\sqrt{r^2 - b^2}} F(\gamma,b) \tag{4}$$

$$N \equiv \int_0^{R_0} n(r)\, 2\pi r\, dr = 4\pi c^2 \int_{-R_0}^{R_0} db \sqrt{R_0^2 - b^2} \int_1^{\infty} d\gamma \, \gamma F(\gamma,b) \tag{5}$$

If we choose $r(\tau) = R_o$ when $\tau = 0$, the radial bounce motion can be parametrized as

$$r^2(\tau) = \begin{cases} b^2 + \left(\sqrt{R_0^2 - b^2} - v|\tau|\right)^2 , & 0 < |\tau| < T/4 \quad (6) \\ b^2 + \left(v|\tau| - \sqrt{R_0^2 - b^2}\right)^2 , & T/4 < |\tau| < T/2 \quad (7) \end{cases}$$

where $v^2 = c^2(\gamma^2 - 1)/\gamma^2$ and T is the time required to complete the bounce motion shown in Fig.2b;

$$T \equiv \frac{2\pi}{\omega_b} = \frac{4}{v}\sqrt{R_0^2 - b^2} \tag{8}$$

We could equally well have chosen half this time, i.e., the time required to go from $r = |b|$ out to $r = R_0$ and back to $r = |b|$ as the fundamental period time for the radial bounce motion, but the choice (8) has the advantage that the change in θ in the time T (denoted by $\Delta\theta$ in Fig.2b) is slow if the impact parameter $|b|$ is much less than R_0

$$\Delta\theta = -2 \tan^{-1}\left(\frac{2b\sqrt{R_0^2 - b^2}}{R_0^2 - 2b^2}\right) \approx -\frac{4b}{R_0} \tag{9}$$

The rapid θ-variation, on the other hand, can be found from

$$r(\tau)e^{i\theta(\tau)} = x(\tau) + iy(\tau) = \begin{cases} e^{i\theta_0}(R_0 + v\tau e^{i\Delta\alpha}) & , \quad -T/2 < \tau < 0 \\ e^{i\theta_0}(R_0 - v\tau e^{-i\Delta\alpha}) & , \quad 0 < \tau < T/2 \end{cases} \tag{10}$$

where $\theta(\tau) = \theta_0$ when $\tau = 0$ and

$$\Delta\alpha = \sin^{-1}(\frac{b}{R_0}) = -\frac{\Delta\theta}{4}$$

The relation $4\Delta\alpha = -\Delta\theta$ is a well known result from Eucledian geometry. We thus have $\theta(\tau) = \theta_0 + \tilde{\theta}(\tau) + \omega_D \tau$, where $\omega_D = \Delta\theta/T$ is the slow drift frequency and $\tilde{\theta}(\tau)$ is a periodic function of τ with period T. Note that the choice $r(0) = R_0$ gives the time reversal relations $r(-\tau) = r(\tau)$ and $\tilde{\theta}(-\tau) = -\tilde{\theta}(\tau)$.

III. Quadratic Form

In solving the Vlasov equation, we shall assume that there is no explicit z-dependence or v_z-dependence in the response function. This procedure has formally been justified in Ref.7 for the interchange mode, by introducing an adiabatic invariant and showing that z-independent perturbations in the particle containment region is an allowable eigenfunction. The identical procedure would work also here, and leads to results that are identical with the following simplified procedure.

We shall neglect electromagnetic wave perturbations. A zero frequency electrostatic mode is certainly justified. However, at finite frequency the accuracy of the electrostatic approximation is questionable for too high a frequency. To justify an electrostatic wave we need δ/c, where δ is the structural distance of an eigenfunction, to be short compared to the wave period. The restrictions of this constraint may be important for relativistic ions, but for simplicity we neglect electromagnetic considerations in this work. At any event, for low harmonics and modes localized near the axis, the electrostatic approximation is justified.

For electrostatic perturbations we take the perturbed potential in the plasma to be

of the form

$$\phi = \hat{\phi}(r)\ exp[\ i(l\theta - \omega t)\ ] \tag{11}$$

The equilibrium distribution function F_0 is a function of the constants of motion, the energy $H = \gamma m_i c^2$ and the angular momentum P_θ, i.e., $F_0 = F_0(H,P_\theta)$. The Vlasov equation for the perturbed distribution, $f_1 = \hat{f}_1(r,\mathbf{v})\ exp[\ i(l\theta - \omega t)\ ]$, is

$$\frac{df_1}{dt} = q_i [\ \frac{\partial F_0}{\partial H}\frac{d\hat{\phi}}{dt} + i(\omega\ \frac{\partial F_0}{\partial H} + l\frac{\partial F_0}{\partial P_\theta})\ \phi\ ] \tag{12}$$

$$\frac{d}{dt} = -i\omega + il\ \dot{\theta} + \dot{r}\frac{\partial}{\partial r} + \ddot{r}\frac{\partial}{\partial \dot{r}}$$

where $\ddot{r} = -2\dot{r}\delta(r-R_0)$. We change the constants of motion to $\gamma = H/m_i c^2$ and $b = P_\theta/[\ m_i c(\gamma^2-1)^{1/2}]$ and define $F(\gamma,b) = F_0(H,P_\theta)$. Then

$$\frac{\partial F_0}{\partial H} = \frac{1}{m_i c^2}(\frac{\partial F}{\partial \gamma} - \frac{\gamma b}{\gamma^2 - 1}\frac{\partial F}{\partial b}) \qquad ; \qquad \frac{\partial F_0}{\partial P_\theta} = \frac{1}{m_i c\sqrt{\gamma^2 - 1}}\frac{\partial F}{\partial b}$$

Now integrating equation (12) yields

$$\hat{f}_1 = \frac{q_i}{m_i c^2}(\frac{\partial F}{\partial \gamma} - \frac{\gamma b}{\gamma^2 - 1}\frac{\partial F}{\partial b})\ (\ \hat{\phi} + i\omega\hat{\Gamma}\ ) + il\frac{q_i}{m_i c\sqrt{\gamma^2 - 1}}\frac{\partial F}{\partial b}\hat{\Gamma} \tag{13}$$

$$\hat{\Gamma}(\mathbf{r},\mathbf{v}) = \int_{-\infty}^{t} d\tau\ \hat{\phi}[r(\tau)]\ exp\{\ il[\theta(\tau) - \theta] - i\omega(\tau - t)\ \} \tag{14}$$

where $\theta = \theta(t)$. We separate out from $\theta(\tau)$ the slow drift motion. The integrand in (14) is then written as

$$\tilde{G}(\tau)\ exp\ [\ -il(\theta - \theta_0 - \omega_D\tau) - i\omega(\tau - t)\ ] \tag{15}$$

$$\omega_D \equiv \frac{\Delta\theta}{T} \approx -\frac{vb}{R_0^2} \tag{16}$$

The oscillating function $\tilde{G}(\tau)$ is a periodic function with period T and is given by

$$\begin{aligned} \tilde{G}(\tau) &= \hat{\phi}[r(\tau)]\ exp\ \{\ il[\theta(\tau) - \theta_0 - \omega_D\tau]\ \} \\ &= \frac{\hat{\phi}(r)}{r^l}\ \{\ [x(\tau) + iy(\tau)]\ e^{\ -i(\theta_0 + \omega_D\tau)}\ \}^l \end{aligned} \tag{17}$$

where we have used $r^{i\theta} = x + iy$ and τ as a function of r and v_r can be found by inverting equations (6) and (7). We Fourier expand $\tilde{G}(\tau)$ in the bounce frequency ω_b

$$\tilde{G}(\tau) = \sum_{n=-\infty}^{\infty} G_n(\gamma,b) e^{\ in\omega_b\tau} \tag{18}$$

$$G_n(\gamma,b) \equiv \frac{1}{T}\oint_{-T/2}^{T/2} \tilde{G}(\tau)\ e^{\ -in\omega_b\tau}\ d\tau \tag{19}$$

Equations (8),(10) and (19) give with $r(-\tau) = r(\tau)$

$$G_n = \frac{v}{\sqrt{R_0^2 - b^2}} \int_0^{T/2} d\tau\ \frac{\hat{\phi}[r(\tau)]}{[r(\tau)]^l}\ Re\Big[\ \frac{1}{2}\ (R_0 - v\tau e^{\ -i\Delta\alpha})^l\ e^{\ -i(\ l\omega_D + n\omega_b)\tau}\ \Big] \tag{20}$$

It is convenient to transform from τ to r, wherein

$$v\tau(r) = \begin{cases} v\tau_1 = \sqrt{R_0^2 - b^2}\ -\ \sqrt{r^2 - b^2}\ , & 0 \le \tau \le T/4 \\ v\tau_2 = \sqrt{R_0^2 - b^2}\ +\ \sqrt{r^2 - b^2}\ , & T/4 \le \tau \le T/2 \end{cases}$$

Using $cos(\Delta\alpha) = (1 - b^{\ 2}/R_0^2)^{1/2}$, $\Delta\theta \equiv \omega_D T$, $\omega_b = 2\pi/T$, $v\,T/2 = 2R_0 cos(\Delta\alpha)$,

$\tau_2(r) = T/2 - \tau_1(r)$ and $4\Delta\alpha = -\Delta\theta$ equation (20) thus takes the form

$$G_n(b) = \frac{1}{\sqrt{R_0^2 - b^2}} \int_{|b|}^{R_0} dr \, \frac{r^{1-l}\hat{\phi}(r)}{\sqrt{r^2 - b^2}} Re[\, h(\tau_1) + (-1)^{n+l} h^*(\tau_1)\,] \tag{21}$$

where * denotes complex conjugate and

$$\begin{aligned} h(\tau_1) &= \frac{1}{2}\left(R_0 - v\tau_1 e^{-i\Delta\alpha}\right)^l e^{-i(n\omega_b + l\omega_D)\tau_1} \\ &= \frac{1}{2}\left(\sqrt{r^2 - b^2} + ib\right)^l exp[-i\frac{n\pi}{2} + i(l\omega_D + n\omega_b)\frac{\sqrt{r^2 - b^2}}{v}] \end{aligned} \tag{22}$$

Note that G_n is real if $\hat{\phi}(r)$ is real, and because $v\tau_1, \omega_D\tau_1$ and $\omega_b\tau_1$ depend on b and are independent on γ, G_n depends on b but not on γ. For $l = 0$, equations (21) and (22) yield the exact relations $G_n(-b) = G_n(b)$, $G_{2n-1} = 0$ and $G_{-2n}(b) = G_{2n}(b)$. Also note that $h(r=R_0) = (R_0)^l/2$. This simplicity at the endpoints indicates that $h(\tau_1)$ can be extended to a periodic function of period T, when τ is extended beyond the domain $0 < \tau < T/4$.

In the limit $b/R_0 \rightarrow 0$, equations (21) and (22) simplify to

$$G_{2n}(b) = \frac{1 + (-1)^l}{2}\frac{(-1)^n}{R_0}\int_{|b|}^{R_0} \frac{r\hat{\phi}(r)}{\sqrt{r^2 - b^2}} cos(n\pi\frac{r}{R_0})\, dr + O(\frac{b}{R_0})$$

$$G_{2n+1}(b) = \frac{1 - (-1)^l}{2}\frac{(-1)^n}{R_0}\int_{|b|}^{R_0} \frac{r\hat{\phi}(r)}{\sqrt{r^2 - b^2}} sin[(2n+1)\frac{\pi}{2}\frac{r}{R_0}]\, dr + O(\frac{b}{R_0}) \tag{23}$$

Further simplification is obtained by assuming that $\hat{\phi}(r)$ is localized near the origin. Then $G_{2n+1} \approx 0$, while

$$G_{2n} \approx \frac{1+(-1)^l}{2}\frac{(-1)^n}{R_0}\int_{|b|}^{R_0}\frac{r\hat{\phi}(r)}{\sqrt{r^2-b^2}}dr \approx (-1)^n G_0$$

If $|\nabla\phi| > |\phi/b|$ near the axis, it is necessary to exclude the region $r < |b|$ from the integration domain.

For odd l - numbers equation (23) gives $G_0(b) = O(b/R_0)$, hence all odd l - modes have a much smaller low frequency response than even l-modes if the mode structure has a radial width larger than $|b|$. Hence it appears that for this orbit configuration even low frequency modes are more important than odd low frequency modes. We further note that a finite edge produces an additional ω_D roughly given by vr_L/R_0^2 (r_L is the Larmor radius at the edge.) Thus if $r_L > |b|$ our model of infinite B at the edge needs to be modified. However, for the $l = 0$ mode which is our primary interest in this work this aspect is not important as $l\Delta\theta$, the parameter that appears in the theory, is zero.

Substituting (15),(16) into (13) give for $\hat{f}_1$

$$\begin{aligned}\hat{f}_1 = {} & \frac{q_i}{m_i c^2}\left(\frac{\partial F}{\partial \gamma} - \frac{\gamma b}{\gamma^2-1}\frac{\partial F}{\partial b}\right) \\ & \times\left\{\hat{\phi} - \sum_{n=-\infty}^{\infty}\frac{\omega G_n(b)}{\omega - l\omega_D - n\omega_b} exp[-il(\theta-\theta_0-\omega_D t) + in\omega_b t]\right\} \\ & - l\frac{q_i}{m_i c\sqrt{\gamma^2-1}}\frac{\partial F}{\partial b}\sum_{n=-\infty}^{\infty}\frac{G_n(b)}{\omega - l\omega_D - n\omega_b} exp[-il(\theta-\theta_0-\omega_D t) + in\omega_b t]\end{aligned} \tag{24}$$

Although it is justified to neglect B for the ions in the containment region, the magnetic field can be crucial for the electrons, as their gyroradii can still be small compared to the characteristic impact parameter. To describe the electron response, we consider a cold electron fluid with the linearized momentum balance equation given by

$$\omega^2 \mathbf{v}_e = i\omega \frac{e}{m_e} \nabla\phi - i\omega\omega_{ce}(r)\, \mathbf{v}_e \times \mathbf{e}_z \tag{25}$$

The continuity equation for the perturbed line-integrated electron density is

$$i\omega\, n_{e,1} = \frac{1}{r}\frac{\partial}{\partial r}[rn(r)v_{e,r}] + il\frac{n(r)}{r} v_{e,\theta} \tag{26}$$

where $n(r)$ is given by equation (4), i.e., quasineutrality is assumed for the equilibrium. Eliminating $\mathbf{v}_e$ from (26) by means of (25) gives a relation between the perturbed electron density and the perturbed electric potential

$$\hat{n}_{e,1} = \frac{e}{m_e}\left\{ \frac{1}{r}\frac{\partial}{\partial r}\left[rn(r) \frac{\frac{d\hat{\phi}}{dr} + \frac{l}{r}\frac{\omega_{ce}}{\omega}\hat{\phi}}{\omega^2 - \omega_{ce}^2(r)} \right] - n(r) \frac{\frac{l^2}{r^2}\hat{\phi} + \frac{l}{r}\frac{\omega_{ce}}{\omega}\frac{d\hat{\phi}}{dr}}{\omega^2 - \omega_{ce}^2(r)} \right\} \tag{27}$$

The Poison equation for ϕ, if the axial length of the disk approaches zero, is

$$\varepsilon_0 \nabla^2\phi = -(q_i n_{i,1} - e n_{e,1})\, \delta(z) \tag{28}$$

Multiplying (28) with the adjoint[8] function $\phi^\dagger = \hat{\phi}(r,z)exp[\, -i(l\theta - \omega t)\,]$, gives after integration over vacuum and plasma regions the quadratic form

$$L(\phi,\phi^\dagger) = L_f + L_e + L_i \equiv 0 \tag{29}$$

The quantities L_f, L_e and L_i are the field energy, the ion and electron response, respectively

$$L_f = \int_0^\infty dr\, 2\pi r \int_{-\infty}^{\infty} dz\, \varepsilon_0 \nabla[\hat{\phi}(r,z)e^{-il\theta}] \nabla[\hat{\phi}(r,z)e^{il\theta}] \tag{30}$$

$$L_e = -\frac{e^2}{m_e}\int_0^{R_0} \frac{dr\,2\pi r\; n(r)}{\omega^2 - \omega_{ce}^2(r)}\left[\left(\frac{d\hat{\phi}}{dr}\right)^2 + \frac{l^2}{r^2}\hat{\phi}^2 + \frac{l}{r}\frac{\omega_{ce}}{\omega}\frac{d}{dr}(\hat{\phi}^2)\right] \tag{31}$$

$$L_i = -q_i \int_0^{R_0} dr\, 2\pi r\, \hat{\phi}(r) \int_{-\infty}^{\infty} d(\gamma v_r) \int_{-\infty}^{\infty} d(\gamma v_\theta)\, \hat{f}_1 \tag{32}$$

A use of a quadratic form is convenient since the exponentials occurring in (24) will not appear in $L(\phi,\phi^{\dagger})$. This can be demonstrated by following the proof given in Ref.8. One uses' the transformation $[r(t_j),\gamma v_r,\gamma v_\theta] \rightarrow (t_j,\gamma,b)$, where the functions $t_j(r)$ are found by inverting equations (6) and (7). The index j goes from -2 to +2 and $0 \le \pm t_{\pm 1}(r) \le T/4$ and $T/4 \le \pm t_{\pm 2}(r) \le T/2$. With $r_j \equiv r(t_j)$, one obtains by evaluating the Jacobian of the transformation $(\gamma v_r, \gamma v_\theta) \rightarrow (\gamma,b)$ and changing the order of integration

$$\begin{aligned} L_i &= -q_i \sum_{j=-2}^{2} \frac{1}{4} \int_0^{R_0} dr_j\, 2\pi r_j\, \hat{\phi}(r_j) \int_{-r}^{r} db \int_1^{\infty} d\gamma\, \frac{2c^2\gamma}{\sqrt{r_j^2 - b^2}}\, \hat{f}_i(\gamma,b,t_j) \\ &= -\pi c^2 q_i \int_{-R_0}^{R_0} db \int_1^{\infty} d\gamma \sum_{j=-2}^{2} \int_{|b|}^{R_0} dr_j\, \frac{r_j}{\sqrt{r_j^2 - b^2}}\, \gamma\, \hat{\phi}(r_j)\, \hat{f}_1(\gamma,b,t_j) \end{aligned} \tag{33}$$

The substitution $r_j \rightarrow t_j(r)$ transforms the sum over the last integrals to a time-integral over the bounce period T

$$L_i = -4\pi c^2 q_i \int_{-b}^{b} db \int_1^{\infty} d\gamma\, \gamma\sqrt{R_0^2 - b^2}\, \frac{1}{T}\oint_{-T/2}^{T/2} dt\, \hat{\phi}[r(t)]\, \hat{f}_1(\gamma,b,t) \tag{34}$$

Equation (24) for $\hat{f}_1$ is now substituted into the time integral in (34)

$$\frac{q_i}{m_i c^2}\left(\frac{\partial F}{\partial \gamma} - \frac{\gamma b}{\gamma^2 - 1}\frac{\partial F}{\partial b}\right)\left[\frac{1}{T}\oint_{-T/2}^{T/2}\hat{\phi}^2(t)\,dt - \sum_n \frac{\omega G_n}{\omega - \Omega_{ln}}\frac{1}{T}\oint_{-T/2}^{T/2}\tilde{G}(-t)e^{in\omega_b t}\,dt\right]$$

$$- l\frac{q_i}{m_i c\sqrt{\gamma^2 - 1}}\frac{\partial F}{\partial b}\sum_n \frac{G_n}{\omega - \Omega_{ln}}\frac{1}{T}\oint_{-T/2}^{T/2}\tilde{G}(-t)e^{in\omega_b t}\,dt \qquad (35)$$

where $\Omega_{ln} = l\omega_D + n\omega_b$ and we have identified $\tilde{G}(-t) = \hat{\phi}[r(t)]\ exp[-il\tilde{\theta}(t)]$, which follows from the definition (17) of $\tilde{G}(t)$ and the time-reversal relations $r(-t) = r(t)$ and $\tilde{\theta}(-t) = -\tilde{\theta}(t)$. The last integral in (35) is equal to $G_n(b)$, as follows from equation (19). The resulting expression for L_i is symmetric, i.e., $L_i(\phi,\phi^\dagger) = L_i(\phi^\dagger,\phi)$:

$$L_i = -4\pi\frac{q_i^2}{m_i}\left\{\int_0^{R_0} dr\, r\hat{\phi}^2\int_{-r}^{r} db\int_1^\infty d\gamma\ \frac{\gamma}{\sqrt{r^2 - b^2}}\left(\frac{\partial F}{\partial \gamma} - \frac{\gamma b}{\gamma^2 - 1}\frac{\partial F}{\partial b}\right)\right.$$

$$- \sum_{n=-\infty}^{\infty}\int_{-R_0}^{R_0} db\sqrt{R_0^2 - b^2}\int_1^\infty d\gamma\ \gamma\left(\frac{\partial F}{\partial \gamma} - \frac{\gamma b}{\gamma^2 - 1}\frac{\partial F}{\partial b}\right)\frac{\omega[G_n(b)]^2}{\omega - l\omega_D - n\omega_b} \qquad (36)$$

$$\left. - l\sum_{n=-\infty}^{\infty}\int_{-R_0}^{R_0} db\sqrt{R_0^2 - b^2}\int_1^\infty d\gamma\ \frac{\gamma c}{\sqrt{\gamma^2 - 1}}\frac{\partial F}{\partial b}\frac{[G_n(b)]^2}{\omega - l\omega_D - n\omega_b}\right\}$$

It is well known that a variation with respect to $\phi^\dagger$ of the quadratic form leads to the Poison equation (28) for ϕ. The choice $\phi^\dagger = \hat{\phi}(r,z)exp[-i(l\theta - \omega t)]$ ensures that L is symmetric[8], $L(\phi,\phi^\dagger) = L(\phi^\dagger,\phi)$, so that $L(\phi,\phi^\dagger)$ is also variational with respect to ϕ. This variational structure allows one to use a testfunction approach to derive approximate stability criteria. If the trialfunction is a first order approximation to the eigenfunction, a second order accuracy[8] is achieved for the eigenvalue by calculating ω from $L(\phi,\phi^\dagger) = 0$.

Let us consider a mono-energetic ion distribution with impact parameters in the range $-b_0 < b < b_1$

$$F(\gamma,b) = n_0 \frac{1}{2\pi c^2}\frac{1}{\gamma_u}\delta(\gamma - \gamma_u)\,\Theta(b_1 - b)\,\Theta(b + b_0) \tag{37}$$

where $n_0 = \int n_v(r=0,z)\,dz$ is the on axis line density and $\Theta(b)$ is the Heaviside function. The particle line density and the total number of particles is given by

$$n(r) = n_0 \sum_{b_i=b0,b1} \left[\frac{\Theta(b_i - r)}{2} + \Theta(r - b_i)\,\frac{1}{\pi}\sin^{-1}\left(\frac{b_i}{r}\right) \right] \tag{38}$$

$$N = 2R_0(b_0 + b_1)n_0 + O\left(\frac{b^2}{R_0^2}\right) \tag{39}$$

With $l = 0$, the ion contribution to the quadratic form can now be expressed as (we write γ instead of γ_u)

$$L_i = -n_0\left[L_i^{(0)}(\phi,\phi^{\dagger}) + \boldsymbol{R}\left(\frac{\omega^2}{\omega_b^2}\right) \right] \tag{40}$$

where $L_i^{(0)}$ is independent of ω

$$L_i^{(0)} = \frac{2q_i^2}{m_i c^2}\sum_{b_i} \left\{ \frac{b_i}{\gamma(\gamma^2 - 1)}\,\eta(b_i) + \frac{1}{\gamma}\int_0^{b_i} b\frac{d\eta(b)}{db}\,db \right\} \tag{41}$$

$$\eta(b) = \int_{|b|}^{R_0} \frac{r\hat{\phi}^2\,dr}{\sqrt{r^2 - b^2}} - \frac{1}{\sqrt{R_0^2 - b^2}}\left(\int_{|b|}^{R_0} \frac{r\hat{\phi}\,dr}{\sqrt{r^2 - b^2}} \right)^2 \geq 0 \tag{42}$$

If the last term in (41) is negligible, which is the case if $(\gamma^2 - 1)b_i^2/R_0^2 << 1$, it follows from the Cauchy-Schwartz inequality that $L_i^{(0)} > 0$ if $\hat{\phi}(r)$ is real. For the frequency-dependent part in (40), one obtains by using the symmetry relations $G_{-2p}(b) = G_{2p}(b)$, $G_{2p}(-b) = G_{2p}(b)$ and $G_{2p+1}(b) = 0$

$$\boldsymbol{R}\left(\frac{\omega^2}{\omega_b^2}\right) = \frac{2q_i^2}{m_i c^2}\sum_{b_i}\left\{\frac{b_i\gamma}{\gamma^2-1}\sqrt{R_0^2-b_i^2}\,S(\gamma,b_i) - \int_0^{b_i}\sqrt{R_0^2-b^2}\left[\frac{S(\gamma,b)}{\gamma}+\frac{\partial S(\gamma,b)}{\partial\gamma}\right]db\right\} \tag{43}$$

$$S(\gamma,b) = 2\,\overline{\omega}^2\sum_{p=1}^{\infty}\frac{[G_{2p}(b)]^2}{p^2-\overline{\omega}^2} \tag{44}$$

$$G_{2p}(b) = \frac{(-1)^p}{\sqrt{R_0^2-b^2}}\int_{|b|}^{R_0}\frac{r\hat{\phi}(r)}{\sqrt{r^2-b^2}}\cos\left(p\pi\sqrt{\frac{r^2-b^2}{R_0^2-b^2}}\right)dr \tag{45}$$

where we have introduced a dimensionless frequency

$$\overline{\omega}(\gamma,b) = \frac{\omega}{2\omega_b} \equiv \frac{\omega}{\pi v}\sqrt{R_0^2-b^2} \approx \frac{\omega}{\pi v}R_0 \equiv \omega_0 \tag{46}$$

It is necessary to know how $\boldsymbol{R}$ is related to the sign of Im(ω) near marginal stability to determine a stability threshold. With $b_i \ll R_0$ and $d\gamma/d\omega_0 = -\gamma(\gamma^2-1)/\omega_0$ one obtains by a partial integration

$$\boldsymbol{R} = \frac{2q_i^2}{m_i c^2}\frac{R_0(b_0+b_1)}{\gamma(\gamma^2-1)}Q(\omega_0)\left[1+O\left(\frac{b_i^2}{R_0^2}\right)\right] \tag{47}$$

$$Q(\omega_0) = 2\omega_0^2\sum_{p=1}^{\infty}\frac{3p^2-\omega_0^2}{(p^2-\omega_0^2)^2}[G_{2p}(0)]^2 \tag{48}$$

If $\omega \to 0$, one finds $\boldsymbol{R} \sim \omega^2$, and thus $L_f - n_0 L_i^{(0)} < 0$ would correspond to a low-frequency instability if $L_e = 0$ and $\hat{\phi}(r)$ is real. It is not clear from (48) whether there are other marginal instability points arising at a finite frequency. It should also be

noted that (47) and (48) are only accurate if the eigenfunction is broader than the density structure, i.e., if $|\nabla\phi| < |\phi / b|$.

A convenient expression for the field energy term L_f can be derived by using the method previously developed in Ref.s 7 and 9. If we neglect any induced charges on surrounding walls [which should be adequate if $\hat{\phi}(r)$ is peaked on axis], we obtain (see appendix A for derivation)

$$L_f = 8\varepsilon_0 \int_0^{R_0} \left\{ \hat{\phi}(0) + s \int_0^s dr \frac{d\hat{\phi}(r)/dr}{\sqrt{s^2 - r^2}} \right\}^2 ds , \qquad l = 0 \tag{49}$$

Note that ϕ in the vacuum region need not be determined to calculate L_f. The procedure to calculate L_f for a disk-shaped plasma can be generalized to arbitrary values of the mode number l. The following formula, in which δ_{l0} stands for Kronecker's δ-symbol, is valid for any integer number l

$$L_f = 8\varepsilon_0 \int_0^{R_0} \left\{ \hat{\phi}(0)\delta_{l0} + s^{1-l} \int_0^s dr \frac{1}{\sqrt{s^2 - r^2}} \frac{d}{dr} [r^l \hat{\phi}(r)] \right\}^2 ds \tag{50}$$

IV. Low-frequency $l = 0$ Modes

We are now in a position to choose a trial function $\hat{\phi}(r)$ and determine a threshold density for the two-stream instability from $L_f + L_e + L_i = 0$. Let us first consider the trial function

$$\hat{\phi}(r) = \begin{cases} 1, & r<\delta \\ \delta/r, & r>\delta \end{cases} \tag{51}$$

This corresponds to an accumulation of net charge in the region $r < \delta$. The function $\hat{\phi}$ given by equation (53) is highly peaked on axis if $b_i << \delta << R_0$. With our trial function the total electrostatic energy is proportional to δ, whereas if the trial function did not fall of as $1/r$ outside the region $r < \delta$ the total electrostatic energy would scale as unity. Therefore, eigenfunctions that do not fall of as $1/r$ have a much larger energy, which is far from the extremizing condition. Assuming $b_i << \delta << R_0$ we obtain from equations (49),(41),(42) and (31) with $\omega = 0$ and B constant

$$\frac{L}{8\varepsilon_0\delta} \approx \pi - 2 - \lambda\left(1 - K_e\frac{R_0^2}{\delta^2}\right) + \lambda\frac{2\gamma^2+1}{18\,\delta^2}\frac{b_o^3+b_1^3}{b_0+b_1} + \lambda\frac{\delta}{R_0}\left[\frac{1}{2}\left(ln\frac{R_0}{\delta}\right)^2 + ln\frac{R_0}{\delta} + 1\right] \tag{52}$$

$$\lambda = \frac{n_0(b_0+b_1)}{\gamma(\gamma^2-1)}\frac{e^2}{2\varepsilon_0 m_i c^2} \approx \frac{N}{2R_0}\frac{1}{\gamma(\gamma^2-1)}\frac{e^2}{2\varepsilon_0 m_i c^2} \tag{53}$$

$$K_e = \frac{\gamma}{6}\frac{m_e}{m_i}\left(\frac{R_g}{R_0}\right)^2 \tag{54}$$

where $R_g = \gamma v\, m_i / eB$ is the ion Larmor radius in the particle containment region and K_e represents the electron response. As $L_e \sim 1/\delta^3$ and $L_i \sim 1/\delta$ the electrons may dominate the particle response for a sufficiently localized perturbation, $(\delta/R_0)^2 < K_e$. This effect can arise because the electrons with their negligible Larmor radii can efficiently sample a localized structure while the ions with their large orbits tend to sample a global structure. This effect can be further amplified for a well focused system. Our calculations assume $\delta << R_0$. This will be fulfilled if $(b_0 + b_1)/R_0 << 1$ and $K_e << 1$. However, in realistic systems the assumption $K_e << 1$ can fail and our analysis then breaks down.

The characteristic length δ for the perturbation is found by making L stationary with respect to variations in δ. One obtains from equation (52)

$$\left(\frac{\delta}{R_0}\right)^3 = \frac{4K_e + \left(\frac{4}{9}\gamma^2 + \frac{2}{9}\right)\frac{b_0^3 + b_1^3}{R_0^2 (b_0 + b_1)}}{\left(ln\frac{R_0}{\delta}\right)^2} \sim 4K_e + \frac{4\gamma^2}{9}\left(\frac{b_i}{R_0}\right)^2 \qquad (55)$$

If $K_e > (\gamma b_i / 3R_0)^2$, one finds that δ is increased compared to the pure ion-ion case (one would get $\delta > R_0$ if $4K_e \gtrsim 1$ which is particularly easy to achieve with relativistic beams), but the threshold is not necessarily strongly modified by the electrons, as $K_e\delta^2 / R_0^2$ still can be small. However, as mentioned earlier, with $R_g \sim 5R_\theta$ a significantly increased threshold is obtained with electrons included.

If $K_e < (2\gamma b_i / 3R_0)^2$, we can neglect the electron response and estimate δ from

$$\frac{\delta}{R_0} \sim \left(\frac{4}{9}\gamma^2 + \frac{2}{9}\right)^{1/3} \left(\frac{b_i}{R_0}\right)^{2/3} \qquad (56)$$

Our assumption that $b_i << \delta << R_0$ imposes a restriction on the impact parameters, $(b_i / R_0)^2 << 9 / (4\gamma^2 + 2)$, which is readily fulfilled for particles with nonrelativistic energies, but can become restrictive in the large γ limit. With the minimizing δ estimated by (56), a threshold particle storage number for the onset of a two-stream ion-ion instability is found from (52) and (53)

$$N \lesssim N_0 \equiv 4\varepsilon_0(\pi - 2)\gamma(\gamma^2 - 1)\frac{m_i c^2}{q_i^2} = 4\varepsilon_0(\pi - 2)\gamma(\gamma + 1)\frac{R_0}{q_i^2}E_{kin} \qquad (57)$$

where $E_{kin} = m_i c^2(\gamma - 1)$ is the kinetic energy of the beam. An alternate form of (57) is $(\overline{\omega}_{pi}/\omega_b)^2 \lesssim \gamma^3 R_0/\Delta Z$, where $\overline{\omega}_{pi}^2 = q_i^2 n_{ave}/\varepsilon_0 m_i$. The threshold (57) only depends on the total number of stored particles and on the energy γ. The low frequency two-stream instability does therefore allow for a very high density near the axis. This favorable scaling for highly focused systems is a result of the reduction of the particle threshold of the relativistic two-stream due to the geometrical focusing in the radial and axial directions. In fact, the particle threshold due to equilibrium limitations, such as overfocusing[8], seems more restrictive than the low frequency

ion-ion two-stream instability for relativistic systems. The limitation in particle staorage number in the Exyder due to overfocusing may be best expressed in terms of the luminosity L defined as $L \equiv c \int n^2 d^3x$. For a completlely neutralized Exyder, the condition is

$$L < \frac{\varepsilon_2 \, ln(R_0/|b|) \, \gamma B_0^4}{2\pi \, [ln(\varepsilon_1)]^2 \, \omega_{ci}^3 \, m_i^2} \tag{58}$$

where B_0 is the edge magnetic field and $\varepsilon_1 = (\omega_{ci}\Delta Z/\gamma v) + |b|/R_0$.The ratio of the threshold (57) to the limitation in particle number due to overfocusing is roughly

$$\frac{N_0}{N_{o\text{-}f}} \approx \frac{\pi - 2}{\pi} (\gamma^2 - 1) \frac{|ln(\Delta Z/r_L)|}{\Delta Z/r_L} \tag{59}$$

where r_L is the Larmor radius at the outer turning point. For energies relevant to antiproton production (i.e., only $E_{kin} \approx 10$ GeV or $\gamma \approx 10$ in a migma[10]) diamagnetic limitations due to overfocusing could thus be more restrictive than the criterion (57).

For strongly relativistic energies, the critical particle number (57) goes as γ^3, which in slab geometry would correspond to propagation parallel to the beam direction. The γ^3 dependence can be traced back to the result that the trial function (51) minimizes L if $b_i << \delta << R_0$, which mainly corresponds to longitudinal propagation.

V. Finite Frequency Instabilities

With $L_e = n_0 L'_e$, our dispersion relation is

$$L(\phi,\phi^\dagger) = L_f - n_0[L_i^{(0)} + \boldsymbol{R} - L'_e] = 0 \tag{60}$$

where $L_f, L_i^{(0)}, \boldsymbol{R}$ and L'_e are independent of n_0. If we again consider the trial function given by equation (51) and assume B = constant and $b_i < \delta < R_0$, we can evaluate

L'_e from equations (31) and (38)

$$L'_e = \frac{e^2}{m_e} \frac{1}{\omega_{ce}^2 - \omega^2} [\, g(b_0) + g(b_1) \,] \tag{61}$$

$$g(b) = \sin^{-1}\left(\frac{b}{\delta}\right) + \frac{1}{2}\frac{\delta}{b}\left[\sqrt{1 - \frac{b^2}{\delta^2}} - \frac{\delta}{b}\sin^{-1}\left(\frac{b}{\delta}\right)\right]$$

$$- \frac{\delta^2}{R_0^2}\left\{\sin^{-1}\left(\frac{b}{R_0}\right) + \frac{1}{2}\frac{R_0}{b}\left[\sqrt{1 - \frac{b^2}{R_0^2}} - \frac{R_0}{b}\sin^{-1}\left(\frac{b}{R_0}\right)\right]\right\}$$

We may consider L as a function of ω, δ and n_0, i.e., $L = L(\omega, \delta, n_0)$. Marginal stability requires $\partial L/\partial\omega = 0$ together with the equation $L = 0$ and the variational condition $\partial L/\partial\delta = 0$. Near any marginal state, one arrives at the dispersion relation

$$(\omega - \omega_m)^2 = 2\,\frac{L_f}{n_0}\frac{\delta n_0}{\partial^2 L/\partial\omega^2}$$

where δn_0 is a small deviation from the density threshold and ω_m is the frequency of the marginal solution. If $\partial^2 L/\partial\omega^2 < 0$ a density increase produces an instability while if $\partial^2 L/\partial\omega^2 > 0$ a density decrease produces instability. Since equation (48) gives $\partial^2 Q/\partial\omega^2 > 0$ if ω and $\hat{\phi}(r)$ are real, one always obtains $\partial^2 L/\partial\omega^2 < 0$ if $L_e = 0$. Thus this shows for streaming ion-ion instabilities, without electrons, that once instability is reached at a critical density n_0 , the system is unstable for all $n > n_0$.

In principle, if the electrons response is included and if $\partial^2 L/\partial\omega^2 > 0$ at a marginal point, an increase of the density from the threshold value can result in a stable state. This would imply an instability band bounded at low and high densities. However, in detailed computations we did not find any high density stabilizing regime.

As a first attempt to evaluate $Q(\omega_0)$, we consider a trialfunction $\hat{\phi}(r)$ which peaks strongly on axis. To approximate G_{2p} we use $b = 0$ and $G_{2p}(0) \approx (-1)^p G_0(0)$, which seems to be a reasonable approximation in view of Eq.(45), at least up to modestly

large indices p [the approximation is inaccurate for $p\pi\,\delta >> R_0$]. The sum in (48) can now be carried out by residue techniques[11]

$$Q(\omega_0) \approx \langle\phi\rangle^2 2\omega_0^2 \sum_{p=1}^{\infty} \frac{3p^2 - \omega_0^2}{(p^2 - \omega_0^2)^2}$$

$$= \langle\phi\rangle^2 \left\{ 1 - \pi\omega_0 \left[2cot(\pi\omega_0) - \frac{\pi\omega_0}{sin^2(\pi\omega_0)} \right] \right\} \qquad (62)$$

where $\langle\phi\rangle = G_0(0)$. For ω_0 real and positive, it follows from (62) that $Q(-\omega_0) = Q(\omega_0)$, $Q(\omega_0 + 1) > Q(\omega_0)$, $Q(\omega_0) \geq 0$ and $Q(\omega_0) \rightarrow \infty$ if $\omega_0 \rightarrow \infty$ (see Fig.3). If k is an arbitrary positive definite integer, one also finds that $Q(\omega_0) \rightarrow \infty$ as $\omega_0 \rightarrow k$ and that $\partial Q(\omega_{0,k})/\partial\omega_0 = 0$ for some real frequency $\omega_{0,k}$ in each interval $k \leq \omega_{0,k} \leq k+1$. However, since $Q(\omega_0) \rightarrow \infty$ as $\omega_0 \rightarrow \infty$, this crude way of evaluating $Q(\omega_0)$ would indicate (provided the variational condition $\partial L/\partial\delta = 0$ can be satisfied) an extremely low (or even zero) density threshold for high frequency ion-ion instabilities. This is clear, since $n_0\boldsymbol{R} \sim n_0 Q(\omega_0)$ and thus the threshold in particle number $n_0 \sim L_f/Q(\omega_{0,k})$ goes to zero as $\omega_{0,k} \rightarrow \infty$.

To avoid that our approximation gives $Q(\omega_0) \rightarrow \infty$ if $\omega_0 \rightarrow \infty$, we note that a peaked trial function having the form (51) roughly leads to

$$[G_{2p}(0)]^2 \approx \begin{cases} (\delta/R_0)^2 [\, ln(R_0/\delta)\,]^2 , & p\pi\delta/R_0 << 1 \\ (\delta/R_0)^2 (R_0/p\pi\delta)^4 \, cos^2(p\pi\delta/R_0) , & p\pi\delta/R_0 >> 1 \end{cases}$$

If $\delta/R_0 << 1$, a convenient interpolation formula, with the correct dependencies for small and large p, can be expressed as

$$[G_{2p}(0)]^2 \approx \frac{(\delta/R_0)^2}{\left\{ [ln(R_0/\delta)]^{-1} + \sqrt{2}(p\pi\delta/R_0)^2 \right\}^2} \qquad (63)$$

Using the approximation (63), we again carry out the sum in (48) by residue methods

$$Q(\omega_0) = [\ \frac{\delta}{R_0} ln(\frac{\delta}{R_0})\ ]^2\ [\ 1 - \frac{\pi\omega_0}{(1 + \omega_0^2/z_0^2)^3}(Q_1 + Q_2)\ ] \tag{64}$$

$$z_0 = \frac{2^{-1/4}}{\sqrt{ln(R_0/\delta)}}\frac{R_0}{\pi\delta} \tag{65}$$

$$Q_1 = 2(1 - \frac{\omega_0^2}{z_0^2})\ cot(\pi\omega_0) - \frac{\pi\omega_0(1 + \omega_0^2/z_0^2)}{sin^2(\pi\omega_0)} \tag{66}$$

$$Q_2 = \frac{\omega_0}{z_0}(\frac{9}{2} + 7\frac{\omega_0^2}{z_0^2} + \frac{\omega_0^4}{z_0^4})\ coth(\pi z_0) + (\frac{3}{2} - \frac{\omega_0^2}{z_0^2} - \frac{1}{2}\frac{\omega_0^4}{z_0^4})\frac{\pi\omega_0}{sinh^2(\pi z_0)} \tag{67}$$

The essential modification from Eq.(62) is the appearance of a finite z_o and the factor Q_2 , which is important in the high-frequency regime. For finite z_o , i.e., δ is nonvanishing, it is clear that asymptotically $Q(\omega_{0,k}) \rightarrow 0$ where $\omega_{0,k}$ are the asymptotic frequencies at which $\partial Q/\partial\omega_0 = 0$.

Some results from numerical computations of ω_0, δ and N/N_0 [N_0 is the threshold predicted by equation (57)] at the marginal states from the equations $L = 0$, $\partial L/\partial\omega = 0$ and $\partial L/\partial\delta = 0$ are shown in Tables I-III. More than one marginal state was found in some frequency intervals. In such a case, the tabulated values correspond to the marginal state with the lowest density. The integers in parenthesis are the number of thresholds found (with N positive) in each frequency interval. Only marginal states with $b_i < \delta < R_0$ are considered in the tables.

Table I and IV for ion-ion interactions show thresholds roughly 30 times lower than the zero frequency threshold given by equation (57). The solutions where $\delta \rightarrow |b|$ are suspect as the analysis assumed $\delta >> |b|$. The threshold densities, which scale as γ^3 for ion-ion interactions if $b_i << \delta << R_0$, are typically much larger with high energy particles than with nonrelativistic energies. With a moderately strong B - field, inclusion of electrons enhance the particle number significantly , by a factor of 4 for $\omega = 0$ and $R_g/R_0 = 5$ (compare Table I and II). The zero frequency threshold is increased further with decreasing B, but the finite frequency thresholds can for some harmonics be reduced by a weaker magnetic field (Table II and III). In contrast to the ion-ion case, an increase in harmonic number for ion-electron interactions does not

always give a lower density threshold in the frequency regime $0 \leq \omega_0 < 10$.

The scaling of the thresholds for ion-electron interactions with the beam energy is shown in Fig.4. The critical particle numbers are increasing with beam energy, and for a sufficiently high energy there is a cut-off, i.e., no marginal state could be found in the computations. As an example, no marginal points for the ion-electron modes were found in the frequency interval $0 \leq \omega_0 < 10$ with $R_g/R_0 = 5$ but otherwise the same parameters as in Table IV. Thus relativistic effects seem to increase the threshold even more than the γ^3- scaling predicted from the ion-ion interaction.

For sufficiently high frequencies, one obtains $\delta \sim b_i$, and then it would be necessary to compute $\boldsymbol{R}(\omega^2/\omega_b^2)$ to higher order in b_i/R_0 as well as to know the eigenfunction structure in more detail. Although our choice of trial function is a crude approximation to the eigenfunctions, the results in the tables for nonrelativistic beams nevertheless give some hint that finite frequency two-stream instabilities in the Exyder might lead to a lower density threshold than predicted from solely the zero frequency ion-ion mode. However, reliable stability statements in the regime require a more thorough investigation.

VI. Summary

A formalism to deal with the Vlasov stability of a thin plasma disk in the Exyder has been developed. Compared to a cylindrical shape, a disk-shaped plasma gives an improvement in the two-stream threshold by the factor $R_0/\Delta Z$. The straight line approximation together with the periodicity constraint for the ion orbits is justified for two-stream interactions, but might be an insufficient model to describe the $l = 1$ modes, if the ion Larmor radius r_L near the outer turning points is larger than the typical impact parameter $|b|$. If $r_L << |b|$, on the other hand, no low frequency flute instability could exist in the Exyder, at least if the perturbation is not too strongly localized to the axis, $|\nabla\phi| << |\phi/b|$. The large B - field near the plasma surface would of course be responsible for that improvement in stability.

Our results for low-frequency streaming interactions, given in equation (57), are favorable for systems with small impact parameters, particularly for relativistic

systems where the critical particle storage number goes as γ^3. The threshold in particle number is even further increased by inclusion of electrons. Diamagnetic limitations due to overfocusing seems more restrictive with relativistic beams as pointed out in equation (59). The finite frequency $l = 0$ modes near harmonics of the ion bounce frequency were investigated. Our preliminary study indicates that the finite frequency modes give a significantly lower threshold than the zero frequency case. The thresholds of these modes are quite sensitive to electron dynamics. These modes set the most stringent limitations to stability, but more careful work is needed to check the sensitivity of our results to the accuracy of the test function.

We have only examined the $l = 0$ case in detail as the problem simplifies considerably from finite l -modes as the equations are independent of the particle drifts. However, finite l -modes at finite frequency are expected to be important and further investigation is needed. We should also add that our results are very optimistic for relativistic systems as no stringent limitation on luminosity is provided by the two-stream effect. Even if overfocusing is taken into account, there is still a possibility for a substantial luminosity which is of interest for a storage ring[3]. On the other hand, our results do set limits on non-relativistic systems.

Acknowledgment

This work was supported by U.S. Dept. of Energy Contract No. DE-FG05-80ET-53088.

Appendix: Field Energy of a Disk-Shaped Plasma

In addition to its relevance to the Exyder, the formula (52) for the field energy is also useful in studies of other disk-shaped objects, for instance the accretion disks of interest in cosmological research. It could therefore be worthwhile to present a derivation of equation (19b) in some more detail than given in Ref.7.

The starting points are a perturbation of the form $\phi = \hat{\phi}(r,z)e^{il\theta}$ and the expression for the field energy

$$L_f = \int_0^\infty dr 2\pi r \int_{-\infty}^{\infty} dz\ \varepsilon_0 \nabla[\hat{\phi}(r,z)e^{-il\theta}] \cdot \nabla[\hat{\phi}(r,z)e^{il\theta}]$$

$$= \int_0^{R_0} dr\ 2\pi r\, \hat{\sigma}(r)\hat{\phi}(r) \qquad \text{(A1)}$$

We have here assumed that there is no induced charge on any surrounding wall, and used $\varepsilon_0\nabla^2\phi = -\sigma\delta(z)$, where σ is the induced surface charge on the plasma disk. Variations of ϕ with z inside the thin disk is neglected.

The next step is to use the Coulomb integral for $\hat{\phi}(r)$

$$\hat{\phi}(r) = \frac{1}{4\pi\varepsilon_0}\int_0^{R_0} dr' r'\, \hat{\sigma}(r')I(r,r') \qquad \text{(A2)}$$

$$I(r,r') = \oint_0^{2\pi} \frac{e^{il\varphi}\, d\varphi}{\sqrt{r^2 + r'^2 - 2rr'\cos\varphi}} \qquad \text{(A3)}$$

The substitution $\xi = rr'e^{i\varphi}$ transforms the integral in (A3) to a closed contour integral C encirculating the singular points at $\xi = 0$ and $\xi = min(r^2, r'^2)$

$$I(r,r') = \frac{1}{i(rr')^l} \oint_C \frac{\xi^{l-1/2}\, d\xi}{(d^2-\xi)^{1/2}\,(\xi-a^2)^{1/2}}$$

$$= \frac{2}{(rr')^l} \int_0^{a^2} \frac{\xi_x^{l-1/2}\, d\xi_x}{\sqrt{d^2-\xi_x}\,\sqrt{a^2-\xi_x}} \qquad \text{(A4)}$$

where $d = max(r,r')$, $a = min(r,r')$ and C is the circle $|\xi| = rr'$. The last expression for $I(r,r')$ is obtained by deforming the circle C to the contour C', as shown in Fig.5. With $(\xi - a^2)^{1/2} = i\,|a^2 - \xi_x|^{1/2}$ on C'_1, the analytical continuation is $(\xi - a^2)^{1/2} = -i\,|a^2 - \xi_x|^{1/2}$ on C'_3. The circular segments C'_2 and C'_4 give no contribution to the integral in (A4) if their radii go to zero. With $s = \sqrt{\xi_x}$, we find from (A2),(A4) and by changing the order of integration

$$r^l\,\hat{\phi}(r) = \frac{1}{\pi\varepsilon_0} \int_0^r ds\, \frac{s^{2l}}{\sqrt{r^2-s^2}} \int_s^{R_0} dr'\, \frac{(r')^{1-l}\,\hat{\sigma}(r')}{\sqrt{r'^2-s^2}} \qquad \text{(A5)}$$

It is convenient here to define a function $f(s)$ which is identical to the second integral in (A5);

$$f(s) = \int_s^{R_0} dr\, \frac{r^{1-l}\,\hat{\sigma}(r)}{\sqrt{r^2-s^2}} \qquad \text{(A6a)}$$

$$r^{1-l}\,\hat{\sigma}(r) = -\frac{2}{\pi}\frac{\partial}{\partial r} \int_r^{R_0} ds\, \frac{s f(s)}{\sqrt{s^2-r^2}} \qquad \text{(A6b)}$$

Equation (A6b), the Abel inversion of (A6a), can be derived from the identity

$$\int_r^s \frac{2x\,dx}{\sqrt{s^2-x^2}\,\sqrt{x^2-r^2}} = \pi \qquad \text{(A7)}$$

By substituting (A6a) into (A5), we find that $r^l\hat{\phi}$ is an Abel transform of the

function $s^{2l}f(s)$

$$r^l\hat{\phi}(r) = \int_0^r ds \frac{s^{2l} f(s)}{\sqrt{r^2 - s^2}} \tag{A8a}$$

$$s^{2l} f(s) = 2\varepsilon_0 \frac{\partial}{\partial s} \int_0^s ds \frac{r^{1+l}\,\hat{\phi}(r)}{\sqrt{s^2 - r^2}} \tag{A8b}$$

Equation (A8b) is found by Abel-inverting (A8a). Eliminating $\hat{\sigma}(r)$ from (A1) by using (A6b) gives after a partial integration and a change of the order of integration

$$L_f = 4\Big\{ f(R_0) \int_0^{R_0} \frac{r}{\sqrt{R_0^2 - r^2}} r^l\hat{\phi}(r)\, dr - \int_0^{R_0} ds \frac{\partial f}{\partial s} \int_0^s dr \frac{r}{\sqrt{s^2 - r^2}} r^l\hat{\phi}(r) \Big\} \tag{A9}$$

At this point, it is most convenient to eliminate $r^l\hat{\phi}$ first, and make use of Eq.(A7)

$$L_f = \frac{2}{\varepsilon_0} \int_0^{R_0} ds\, [s^l f(s)]^2 \tag{A10}$$

The final expression is obtained by substituting Eq.(A8b) into (A10)

$$L_f = 8\varepsilon_0 \int_0^{R_0} ds \Big\{ \hat{\phi}(o)\delta_{l0} + s^{1-l} \int_0^s \frac{dr}{\sqrt{s^2 - r^2}} \frac{d}{dr} [r^l\hat{\phi}(r)] \Big\}^2 \tag{A11}$$

This convenient formula shows that it is sufficient to know $\hat{\phi}(r,z)$ at the plasma disk only to determine the field energy. A simple application of Eq.(A11) is the classical problem of determining the charge distribution on an insulated metal disk with net charge Q. Variations of (A11) yields $\sigma(r) = Q/[2\pi R_0(R_0^2 - r^2)^{1/2}]$.

References

1. J.P. Blewett, Nuclear Instr. and Methods **A271**, 214 (1988).

2. J.P. Blewett (to be published) (1988).

3. H.L. Berk and H.V. Wong, Institute for Fusion Studies Report No. 340 (1988).

4. B.C. Maglich, J.P. Blewett, A.P. Colleraine, and W.C. Harrison, Phys. Rev. Lett. **27**, 909 (1971).
5. F.T. Gratton and G. Gnavi, Phys. Fluids **30**, 548 (1987).

6. G. Gnavi and F.T. Gratton, Nuclear Instr. and Methods **A271**, 112 (1988).

7. H.L. Berk and H.V. Wong, Z. Naturforsch. **42A**, 1208 (1987).

8. R.R. Domingues and H.L. Berk, Phys. Fluids **27**, 1142 (1984).

9. H.V. Wong, M.N. Rosenbluth and H.L. Berk, Phys. Fluids B **1**, 826 (1989)

10. B.C. Maglich, Nuclear Instr. and Methods **A271**, 167 (1988).

11. P. Morse and M. Feshbach, Methods of Theoretical Physics, Vol. I, p.419 (1953).

Table I. Marginally stable parameters for nonrelativistic ion-ion interactions (E_{kin} = 1 MeV with protons). The electron response is neglected. The parameter values are $b_0/R_0 = b_1/R_0 = 0.005$.

Frequency range		ω_0	δ/b_0	N/N_0
$0 \leq \omega_0 < 1$	(1)	0	1.87	1.25
$1 < \omega_0 < 2$	(3)	1.391	4.52	0.34
$2 < \omega_0 < 3$	(1)	2.439	3.35	0.16
$3 < \omega_0 < 4$	(3)	3.458	2.58	0.094
$4 < \omega_0 < 5$	(1)	4.468	2.09	0.065
$5 < \omega_0 < 6$	(1)	5.474	1.74	0.049
$6 < \omega_0 < 7$	(1)	6.479	1.50	0.039

Table II. Marginally stable parameters for nonrelativistic electron-proton interactions, E_{kin} = 1 MeV, with $b_0/R_0 = b_1/R_0$ = 0.005, R_g/R_0 = 5 and $K_e = 2.28\times10^{-3}$. The computation is restricted to frequencies well below the electron cyclotron frequency (electron resonance occurs at $\omega_0 \approx 117$).

Frequency range		ω_0	δ/b_0	N/N_0
$0 \le \omega_0 < 1$	(1)	0	30.0	5.13
$1 < \omega_0 < 2$	(1)	1.433	9.90	0.74
$2 < \omega_0 < 3$	(1)	2.466	6.60	0.34
$3 < \omega_0 < 4$	(3)	3.480	5.05	0.22
$4 < \omega_0 < 5$	(3)	4.487	4.15	0.16
$5 < \omega_0 < 6$	(3)	5.491	3.55	0.13
$6 < \omega_0 < 7$	(3)	6.493	3.12	0.11
$7 < \omega_0 < 8$	(1)	7.495	2.81	0.10
$8 < \omega_0 < 9$	(1)	8.497	2.57	0.93
$9 < \omega_0 < 10$	(1)	9.498	2.37	0.88

Table III. Marginally stable parameters for nonrelativistic electron-proton interactions, E_{kin} = 1 MeV, with $b_0/R_0 = b_1/R_0 = 0.005$ $R_g/R_0 = 7$ and $K_e = 4.47\times10^{-3}$.

Frequency range		ω_0	δ/b_0	N/N_0
$0 \le \omega_0 < 1$	(1)	0	40.0	9.20
$1 < \omega_0 < 2$	(1)	1.500	20.0	5.97
$2 < \omega_0 < 3$	(1)	2.480	8.32	0.75
$3 < \omega_0 < 4$	(3)	3.490	6.48	0.52
$4 < \omega_0 < 5$	(3)	4.496	5.42	0.44
$5 < \omega_0 < 6$	(2)	5.499	4.72	0.43
$6 < \omega_0 < 7$	(2)	6.501	4.28	0.47
$7 < \omega_0 < 8$	(2)	7.503	3.92	0.58
$8 < \omega_0 < 9$	(2)	8.504	3.70	0.95
$9 < \omega_0 < 10$	(2)	9.505	3.55	0.48

Table IV. Marginally stable parameters for relativistic proton-proton interactions, E_{kin} = 10 GeV or γ =11.6, with $b_0/R_0 = b_1/R_0$ = 0.005. The electron response is neglected.

Frequency range		ω_0	δ/b_0	N/N_0
$0 \leq \omega_0 < 1$	(17)	0	9.88	2.13
$1 < \omega_0 < 2$	(9)	1.403	6.30	0.39
$2 < \omega_0 < 3$	(1)	2.448	4.32	0.18
$3 < \omega_0 < 4$	(3)	3.464	3.32	0.11
$4 < \omega_0 < 5$	(1)	4.474	2.67	0.077
$5 < \omega_0 < 6$	(1)	5.479	2.26	0.059
$6 < \omega_0 < 7$	(1)	6.483	1.95	0.047
$7 < \omega_0 < 8$	(1)	7.486	1.74	0.039
$8 < \omega_0 < 9$	(1)	8.488	1.57	0.033

Figure Captions

1. a) Geometry of the coil configuration in a Migma Exyder.
   b) Profile of B_z in the (x,y) plane as produced by the coils shown in Fig.1a. Reversal of the field in the central region is obtained in the case $I_2 = -I_1$. (Figure from Blewett, 1988.)

2. a) Outline of orbit shape in the Blewett storage ring. The orbits A and B would be stable while the orbit C would be lost in the axial direction. (Figure from Blewett, 1988.)
   b) Ion orbits used to model the two-stream effect in the Migma Exyder.

3 Plot of the function $Q(\omega_0)/\langle\phi\rangle^2$, where $Q(\omega_0)$ is given by equation (37). $Q(\omega_0)$ is singular whenever $\omega_0 \equiv \omega/2\omega_b = k$, where k is a positive definite integer. The marginal points are the frequencies $\omega_{0,k}$ at which $\partial Q/\partial\omega_0 = 0$. The marginal points nearly intersect with the curve $\pi^2\omega_0^2$ (dashed line).

4. Threshold density for electron ion interactions versus beam energy for the zero frequency mode ($k = 0$) and the first three harmonics ($k = 1,2,3$). The computations were made with $b_0/R_0 = b_1/R_0 = 0.005$ and $R_g/R_0 = 5$.

5. Deformation of the integration contour C to the contour C'. Both curves encircle the branch points at $\xi = 0$ and $\xi = a^2$.

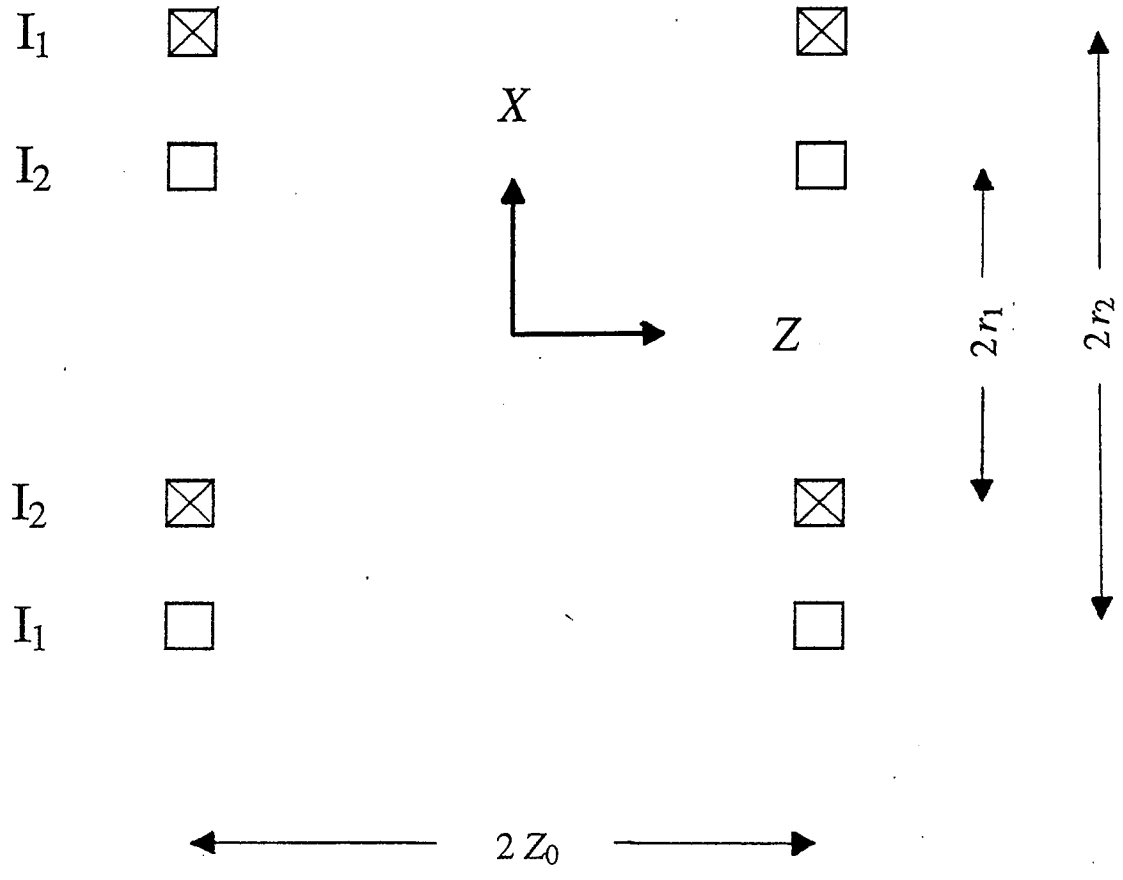

Fig. 1a

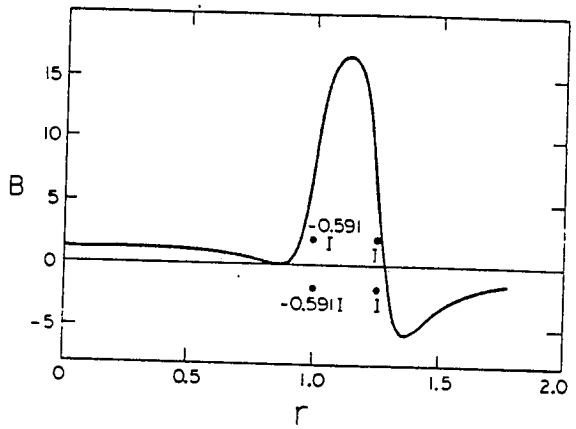
15
10
B
5
0
-5
-0.591
I
I
-0.591 I
I
0
0.5
1.0
1.5
2.0
r

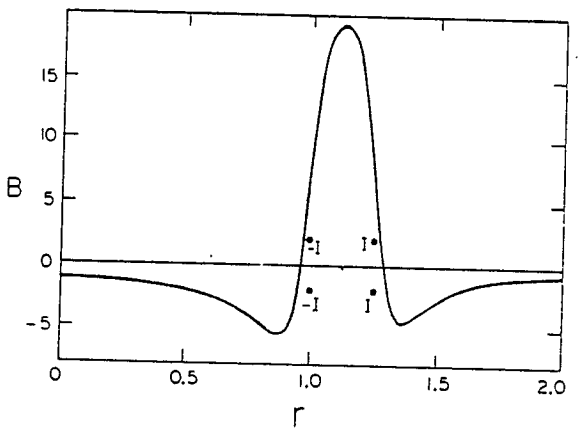
15
10
B
5
0
-5
-I
I
-I
I
0
0.5
1.0
1.5
2.0
r

Figure 1b

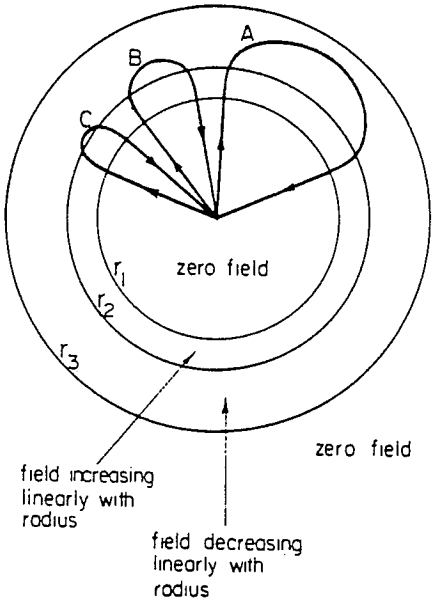
A
B
C
zero field
r_1
r_2
r_3
zero field
field increasing linearly with radius
field decreasing linearly with radius

Figure 2a

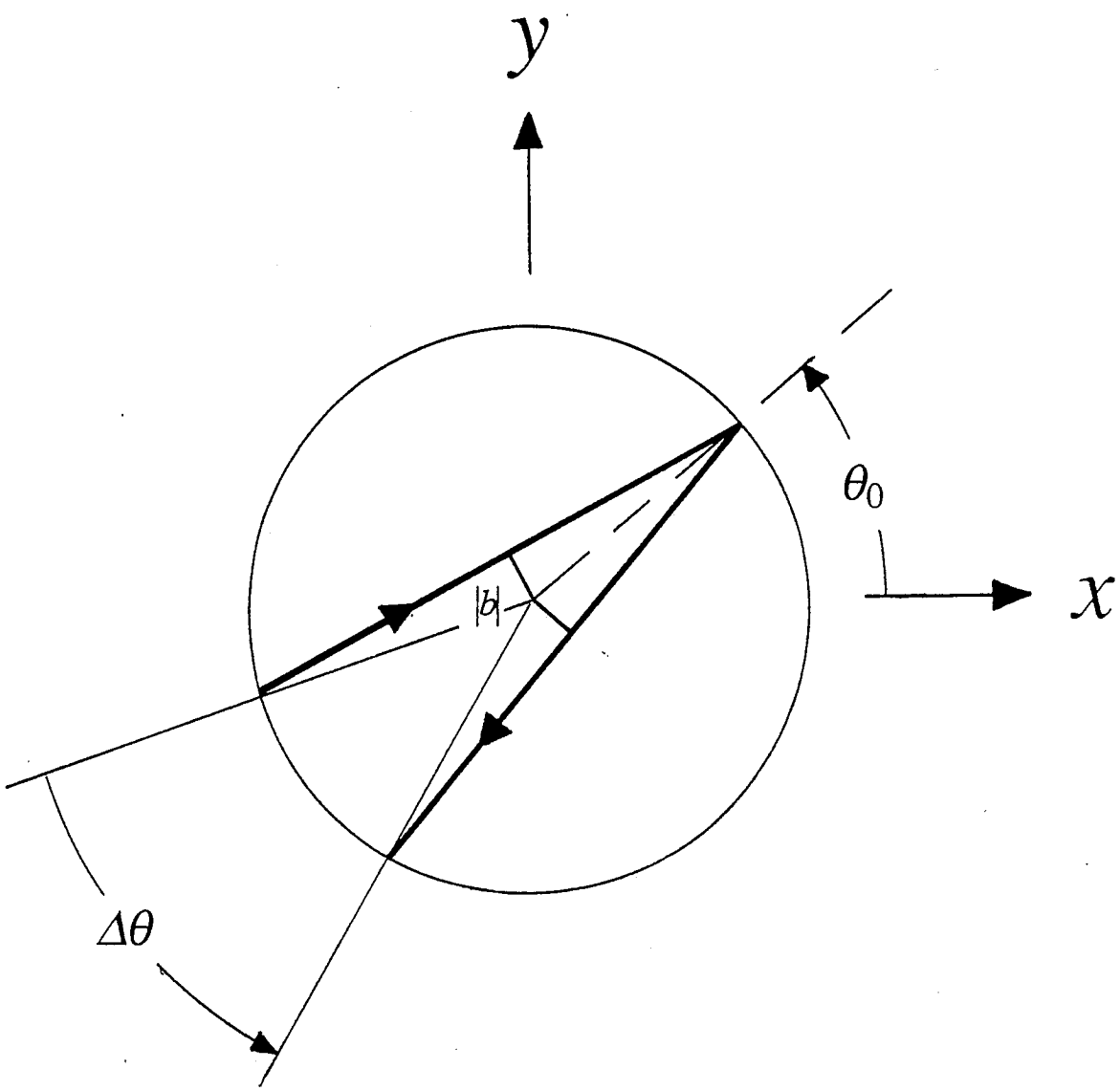

Figure 2b

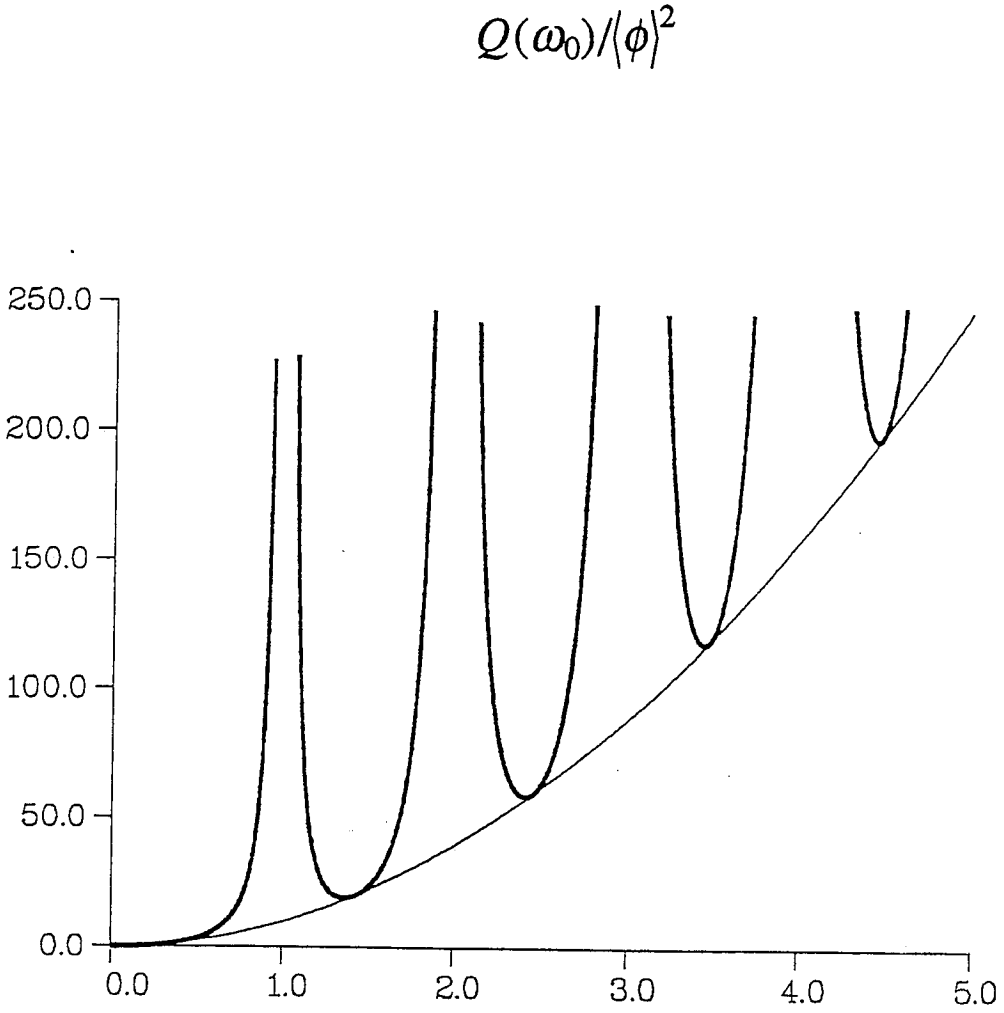

Figure 3.

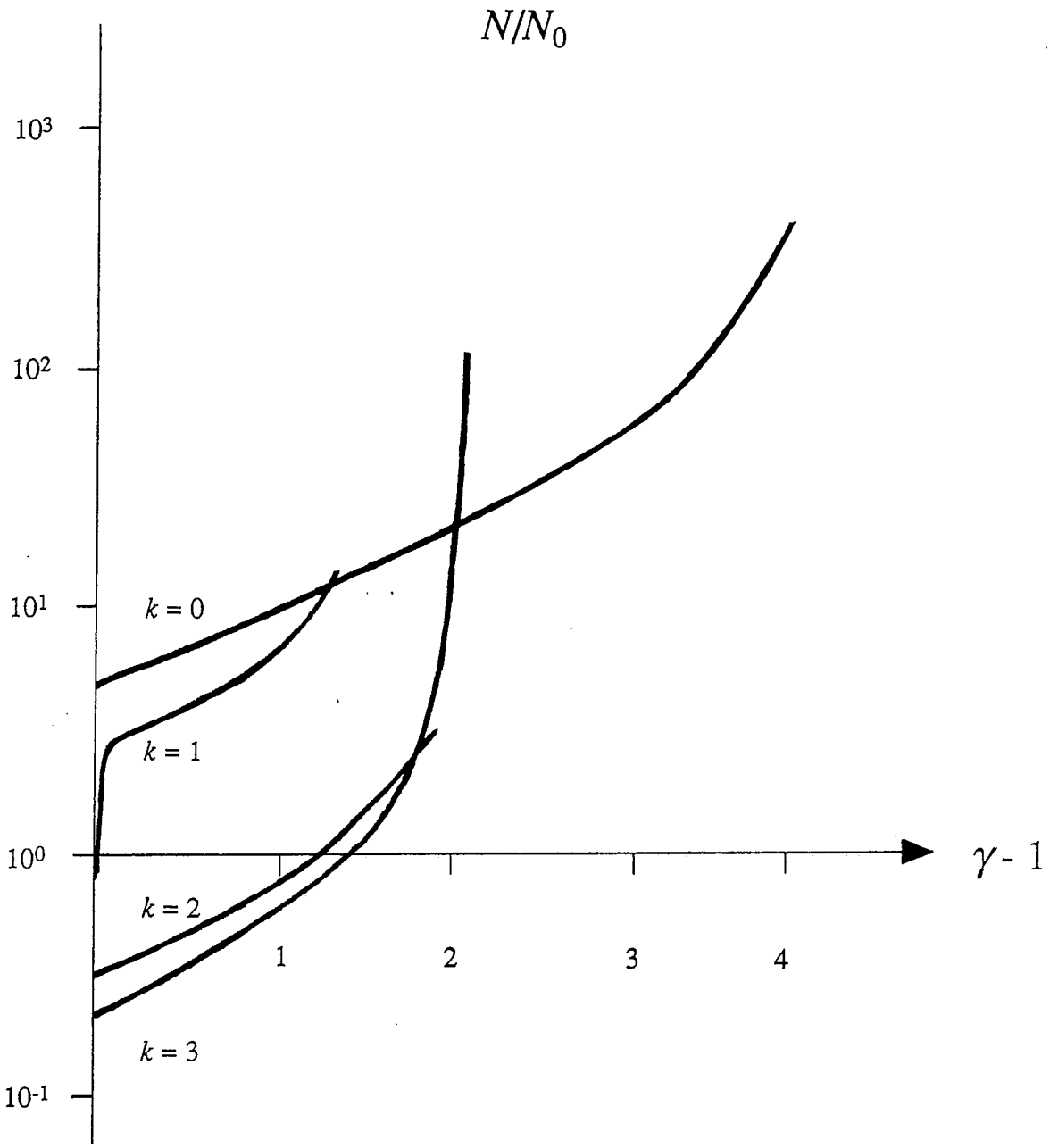

Figure 4.

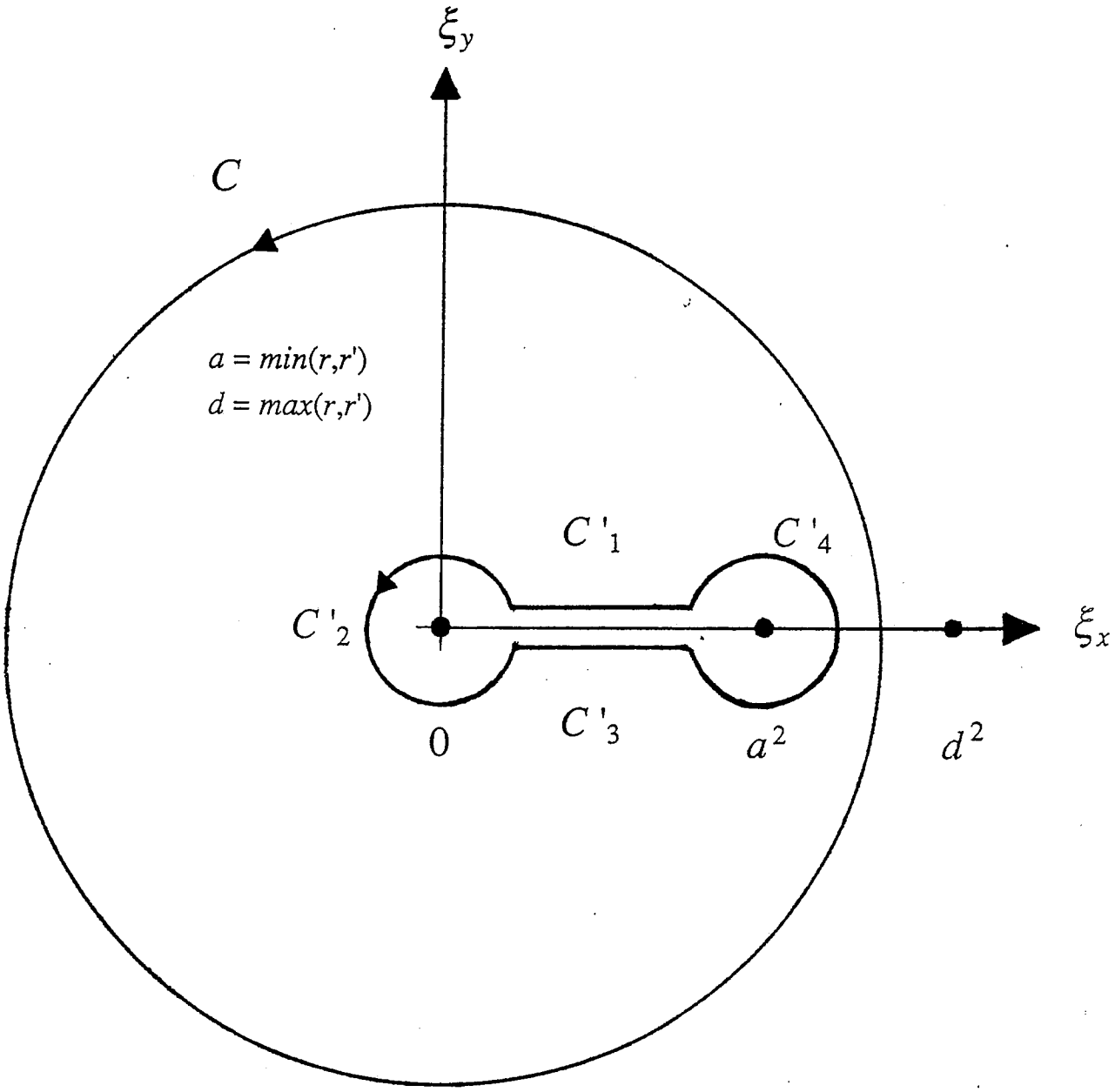

Figure 5.